

Wai Kean Yap

Quantitative Analysis of Dust and Soiling on Solar PV Panels in the Tropics Utilizing Image-Processing Methods

Wai Kean Yap¹, Roy Galet² and Kheng Cher Yeo²

¹*Centre for Renewable Energy, Charles Darwin University, Ellengowan Drive, Darwin 0909
NT, Australia*

²*School of Engineering and IT, Charles Darwin University, Ellengowan Drive, Darwin 0909
NT, Australia*

E-mail: wai.yap@cdu.edu.au

Abstract

Maximizing the efficiency of solar photovoltaic (PV) systems in the unique Northern Australia climate (dry and wet seasons annually) is critical in particular for rooftop installations. Optimum system efficiencies are usually achieved during the dry season, due to consistent sunshine hours, minimal cloud cover and no rainfall. However, the rate of dusting and soiling occurring on the panel surfaces are also high during this period, reducing the system's efficiency. One of the solutions to maintain the optimum efficiency is to clean the panels regularly. However, this was rarely done, especially for rooftop systems due to access problems, and is an added cost. In addition, the cleaning frequency differs from locations and technology types. This paper presents a non-evasive methodology in quantifying the amount of dust and soiling on solar PVs by investigating five different image-processing techniques. This study looks at analyzing color histograms and statistical properties of the captured PV images. An image-processing Toolbox were developed in this study by adopting the following techniques: binarization, histogram model, statistical model, image matching and texture matching. Two image tests were presented: controlled image and actual image tests with average errors of 12.38% and 10.8% were achieved respectively. Results showed that the binarization algorithm exhibited the fastest and the most accurate reading on the controlled image test and the image matching algorithm exhibited the highest accuracy on the actual image test. The methods of analyzing PV panel dusting and soiling were proven to be accurate, low-cost, easy to implement and critically, provides the end-user the necessary information in maintaining their PV system efficiency over the wet and dry seasons of Northern Australia.

1. Introduction

A solar panel system's power output efficiency generally depends on a number of design, environmental and climatic factors such as orientation, sloping angle, shading, and weather. Soiling on solar panel systems, specifically dust from sand and combined dust and moisture formation, have been one of the most underestimated factor that significantly affects the performance of solar panels (Sarver et al., 2013; Qasem et al., 2014; Biryukov et al., 1999; Ndiaye et al., 2013). A recent study by Yap et al. (2014) showed that a roof-integrated

photovoltaic system exhibited a passive reduction on its peak power output even under ideal weather conditions. This study was conducted within Charles Darwin University near Casuarina, Northern Territory, during the dry season. With minimal cloud cover and no rainfall (to naturally clean the panel surface) over this period, Yap et al. (2014) concluded that dust accumulation is one of the primary factors in the decline of the system's efficiency. Results showed a 19.6% and 9.2% for the maximum energy output and 34% and 22% reduction of the total daily energy production for the CIGS and c-Si systems respectively during the dry season period.

Several image processing techniques have already been formulated where its application ranges from object tracking (Perez et al., 2002), pattern recognition (Blanchart et al., 2014), sensors and measurements (Proietti et al., 2014; Santamaria and Malomo, 2014) and quality control in manufacturing (Elbehiery et al., 2007; Parker et al., 2011). The use of image processing in analyzing dust data in PV systems has not been widely explored.

This study will explore relevant image processing techniques used in the literature (Zhang and Subasinghe, 2012; Proietti et al., 2014; Prakongkep et al., 2010; Williams et al., 1998; Lee, 2014) for dust and soiling classification of PV panels. The key factors driving this work are the non-intrusive nature of computer vision and remote sensing systems (Kistner et al., 2013) and improved data acquisition capacity of modern cameras, which are particularly helpful in inaccessible areas, and during unsafe or hazardous operating conditions. Image processing can also reliably replace visual inspection because image processing can analyze colors more consistently and more accurately compared to the human eye (Elbehiery et al., 2007).

2. Methodology

This study explores five different image processing algorithms that can be applied to PV panel images for dust and soiling quantification:

2.1. Binarization (T1) algorithm

Proietti et al. (2014) devised a methodology for dust detection and analysis using a customized sensor to measure the area covered by dust and to count the number of fili-form and circular particles. Proietti et al.'s (2014) method involves five steps: grayscale conversion, background equalization, background removal, binarization, and de-noising. Proietti et al. (2014) claimed the method have a value of correctness of at least 85%. This study, however, emphasizes more on Proietti et al.'s (2014) grayscale and binary conversion processes to lessen the computational effort and since all the other steps are either not applicable or have little effect on the resulting values. As shown on the Fig. 1 below, the white pixels represent the dust particles after the binarization process.

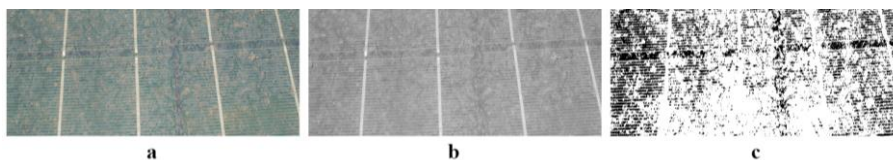


Figure 1. (a) image of a dusty PV panel, (b) image after grayscale conversion, (c) resulting binary image

2.2. Histogram model (T2) algorithm

In the field of industrial mining, Singh et al. (2010) proposed a technique in classifying ores for blast furnace feed. Fig. 2(a) below shows an example of a dusty image and its corresponding histogram. The colour information of dust was extracted from Fig. 3(a) to get the minimum and maximum colour values. On Fig. 3(b) and Fig. 2(c), only a fraction of the total number of pixels fall within the range and can be interpreted as the amount of dust within the image.

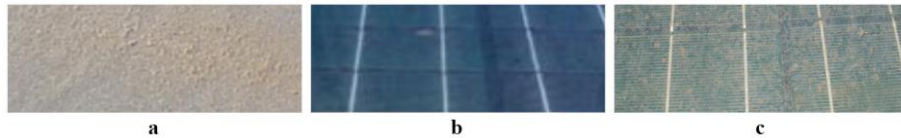


Figure 2. Images of (a) Dust, (b) clean solar panel surface, (c) partly dusty solar panel surface

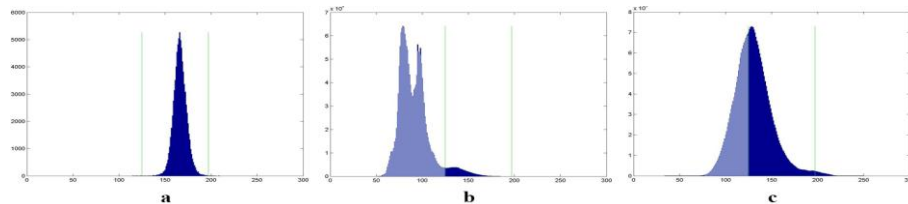


Figure 3. Histograms of (a) Dust, (b) clean solar panel surface, (c) partly dusty solar panel surface

2.3. Statistical model (T3) algorithm

In addition to histogram analysis, Singh et al. (2010) also proposed a statistical method in ore classification. The statistical formulas are based on Haralick et al.'s (1973) measurements of an image's textural features based on the gray level co-occurrence matrix. These properties include entropy, energy, contrast and homogeneity, where the governing equations were shown in Table 1.

In this demonstration, the statistical values of the 11 controlled images were tested using the formulas shown in Fig. 4. Polynomial regression was used on the statistical values to determine the equations for the relationship between each property and the area covered by dust. The resultant dust percentage can then be obtained by determining the real positive roots of the equation of each property.

Table 1. Statistical formulas for 2D spatial grid (images) (Haralick et al., 1973)

Property	Formula
Gray Level Co-Occurrence Matrix	$p(i, j) = \{(r, s), (t, v) : I(r, s) = i, I(t, v) = j\} $
Entropy	$Entropy = - \sum_{i,j} p(i, j) \log p(i, j)$
Energy	$Energy = \sum_{i,j} p(i, j)^2$
Contrast	$Contrast = \sum_{i,j} i - j ^2 p(i, j)$
Homogeneity	$Homogeneity = \sum_{i,j} \frac{p(i, j)}{1 + i - j }$

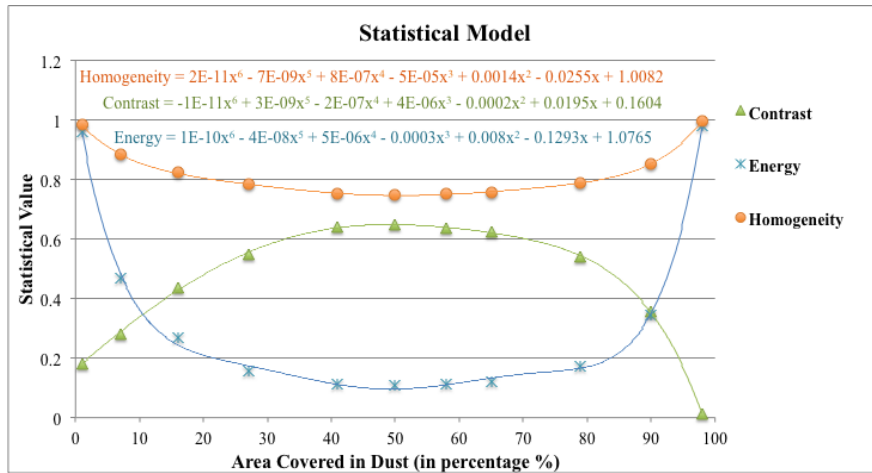


Figure 4. Graph showing the statistical values of controlled images in relation to the area covered in dust

2.4. Color matching (T4) algorithm

Lee (2014) demonstrated a simple but effective method of generating a photomosaic by featuring block-matching which can also be used in detecting dusts which is more effective on photographs of solar panels with uneven dust distribution, or shots taken from wide angle lens or at non-perpendicular angles. In dust detection, the input image is partitioned into rows and columns. Block matching is used in determining the closest match for a specific partition from the collection of smaller images with known dust percentages. The algorithm uses a derived Euclidean equation which calculates the difference of the RGB values between the points in the partition against the points in each image in the database as shown in Equation 1 (Lee, 2014). The known dust coverage percentages of the closest match for each partition will then be averaged to estimate the resulting dust coverage of the larger input image.

$$Difference = \sum_{k=1}^n \sqrt{(R_i - R_j)^2 + (G_i - G_j)^2 + (B_i - B_j)^2} \quad [1]$$

2.5. Texture Matching (T5) algorithm

Williams et al. (1997) have formulated a quantitative method in characterizing quartz sand grains by mathematical analysis of surface texture and were able to correctly classify the quartz sand grains 87.5% of the time. Lee's (2014) photomosaic technique can be adapted to match smaller partitions with the textural features of images stored in the database. Instead of using the RGB channel values, the statistical values for homogeneity, contrast, energy and correlation were used in the Euclidean equation in finding the closest match in the database.

$$Correlation = \sum_{i,j} \frac{(i - \mu_i)(j - \mu_j)p(i,j)}{\sigma_i \sigma_j} \quad [2]$$

2.6. Image Processing Toolbox

The Image Processing Toolbox is the Windows-based application that integrates the algorithms T1 to T5. The toolbox accepts an image file of a solar panel photograph and measures the area of the solar panel surface that is covered in dust. The core of the toolbox contains the algorithms T1 to T5 that are coded as functions using MATLAB and packaged in a single dynamic link library (DLL). The graphical user interface of the toolbox is designed

using Visual Studio 2015 wherein codes are written in C#. The toolbox can run in any computer with at least Windows 7 operating system. The toolbox features intuitive controls and allows customizations such as providing options for users on which algorithms to use in measuring the area covered by dust.

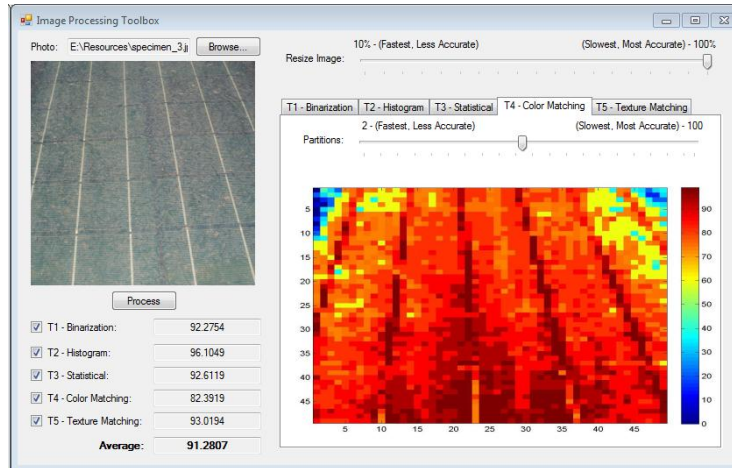


Figure 5. The Windows-based graphical user interface of the Image Processing Toolbox

Performance-wise, large input images add computational complexity and cause the algorithms to process slower. To rectify the problem, options were added to reduce the size of the input image for T1 to T5. On T3, options to exclude statistical equations for Entropy and Energy were added to hasten program execution. For T4 and T5, a setting to reduce the number of partitions has also been included. These settings allow quick measurements, which are beneficial to slower computers at the expense of accuracy, otherwise, higher accuracy can be achieved but requires longer processing times.

3. Results and Discussion

The algorithms were tested on both controlled images and actual photographs. Initially, a set of controlled images shown on Fig. 6 was created resembling a solar panel surface with different amount of light-coloured pixels representing dust particles.

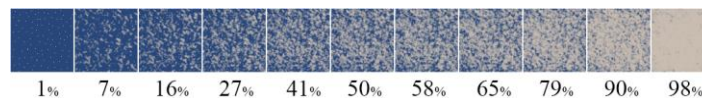


Figure 6. Controlled images with the percentage of area covered in dust

The amount of dust was measured by counting the number of light-coloured pixels that were added to the dark background. Using the Image Processing Toolbox, the algorithms were tested to each of the controlled images to determine the value of correctness and to compare the accuracy levels.

3.1. Controlled image test

The algorithms were fine-tuned to ensure that the results are as close as possible to the correct dust percentages for every test on the controlled images. The same set but smaller versions of controlled images was also used as the database of images for T4 and T5. As expected, the algorithms show high accuracy on the controlled images with maximum average mean

relative error (MRE) of 12.38%. The test on controlled images shows T1 (Binarization) and T3 (Statistical) were the most accurate algorithms. The results are summarized in Table 2.

Table 2. Estimated amount of dust using controlled images

	Controlled Images (%)											MRE (%)
												
	1	7	16	27	41	50	57	65	79	90	98	
T1	1.0	7.6	16.1	27.4	41.4	50.6	58.4	65.4	78.9	90.9	97.9	1.40
T2	1.0	8.3	17.4	29.1	43.5	52.4	60.1	67.0	80.0	91.5	97.9	4.76
T3	1.0	6.9	15.9	27.1	41.5	48.5	59.5	63.5	79.3	89.9	98.0	1.20
T4	1.5	9.7	18.7	29.1	43.7	52.2	59.3	66.1	78.8	88.9	97.9	9.12
T5	2.3	9.7	19.5	29.1	44.6	53.3	58.9	64.5	76.9	87.5	95.3	12.38

3.2. Actual image test

To verify the accuracy of each algorithm, the test was conducted on a 40W Powertech Monocrystalline solar panel, which is commercially available. A 24-megapixel Nikon D3200 DSLR with 18-55mm kit lens was mounted on a tripod and controlled by a computer to avoid shaking. Sand taken from a nearby beach is used in place of dust since the soiling found on the BIPV rig is mostly composed of airborne sand. Initially, two photographs of the solar panel are taken 10 seconds apart while it is still clean. Then, sand is sprinkled onto the surface and another photograph is taken. The process of applying sand is repeated until the solar panel is completely covered.

The percentage of the surface area covered by dust is measured using imageDiff - a pixel-by-pixel image comparison tool developed by ionForge. One advantage of imageDiff compared to similar programs is the feature to display the percentage of pixels that are changed. In the test, imageDiff was used to compare the photographs of the clean, and the dusty solar panel as shown above.

Table 3. Estimated amount of dust using real photographs (%)

Image	Pixels changed ¹ (%)	Area covered by Dust (%)					MRE (%)				
		T1	T2	T3	T4	T5	T1	T2	T3	T4	T5
	98.9	99.6	99.3	99.6	100.0	99.9	0.7	0.4	0.7	1.0	1.0
	89.9	92.6	92.7	95.1	91.0	92.8	2.9	3.0	5.4	1.2	3.1
	79.1	82.9	84.0	83.7	81.9	84.5	4.5	5.8	5.5	3.4	6.4
	53.1	60.1	58.9	56.6	58.8	66.2	11.7	9.9	6.2	9.8	19.8
	44.4	51.9	52.8	48.2	50.5	58.5	14.5	16.0	7.8	12.0	24.1
	30.2	38.3	38.9	33.8	38.3	48.3	21.2	22.2	10.7	21.2	37.5
	21.0	30.3	30.0	25.0	29.5	42.1	30.8	30.1	16.1	29.0	50.2
	7.2	19.1	18.2	11.5	16.9	31.0	62.3	60.5	37.8	57.5	76.9

¹ The percentage of pixels changed was measured using the software imageDiff.

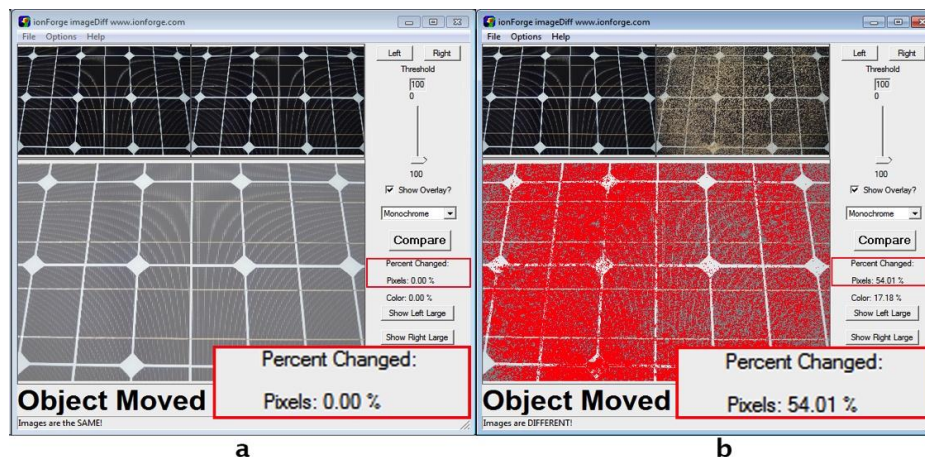


Figure 7. (a) Photographs of the same solar panel taken 10 seconds apart before applying sand (b) Comparison of the photographs after applying sand

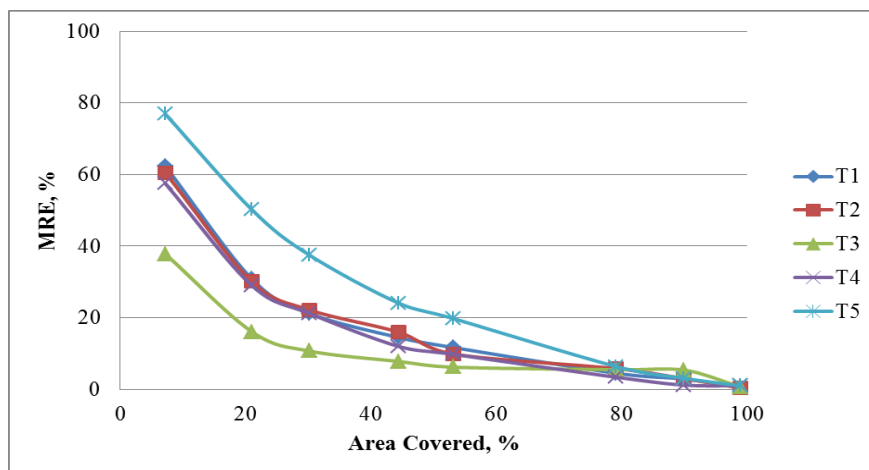


Figure 8. MRE for algorithms T1 – T5

The test was repeated 10 times, which resulted to 100 photographs, but only 40 were randomly selected to undergo comparison test with imageDiff. A batch program was coded in MATLAB to execute T1 to T5 optimized for highest accuracy to the selected 40 photographs. Initial results show higher errors especially on photographs of both clean and with lower dust percentages. This was due to the higher than usual amount of white and gold-colored stripes on specific model of solar panel used in the test, which the Image Processing Toolbox misinterpreted as dust as the colors of the stripes were marginally similar to the color of dust. Error is lower in photographs showing higher amounts of dust because the stripes were mostly covered.

3.3. Error correction analysis

On this model of solar panel, the white and gold colors represent approximately 10% of the whole color map. To solve the problem, error-correction formulas have been determined for each algorithm to reduce the error thus aimed at increasing the accuracy of the algorithms. The error-correction formulas are based on selecting the best-fit line during regression analysis of the initial outputs with the respective deviation from the correct output and applying the resulting formula to the initial outputs. Additionally, instead of using the controlled images as the image database for T4 (Image Matching) and T5 (Texture Matching),

smaller versions of 14 of the unique actual photographs have been used in the matching process when the error-correction formula was implemented.

Table 4. Formulas for the error correction using regression

Algorithm	Regression	Error Correction Formula
T1 - Binarization	Linear	$T1 = T1 - (-0.1239 * T1 + 13.518)$
T2 - Histogram	Linear	$T2 = T2 - (-0.1129 * T2 + 12.806)$
T3 - Statistical	Linear	$T3 = T3 - (-0.0196 * T3 + 5.3645)$
T4 - Image Matching	Linear	$T4 = T4 - (-0.1051 * T4 + 11.903)$
T5 - Texture Matching	Linear	$T5 = T5 - (-0.3374 * T5 + 34.829)$

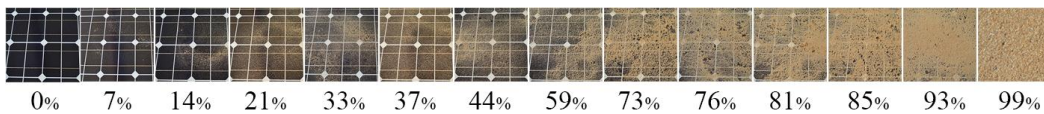


Figure 9. Image database based on actual test photographs and corresponding percent of area covered in dust

Table 5. Estimated amount of dust using real photographs after error-correction (%)

Image	Pixels changed (%)	Results after Error Correction (%)					Mean Relative Error (%)				
		T1	T2	T3	T4	T5	T1	T2	T3	T4	T5
	98.9	98.4	97.7	96.2	98.6	98.8	0.5	1.2	2.8	0.4	0.1
	89.9	90.6	90.4	91.6	88.7	89.3	0.7	0.5	1.8	1.4	0.7
	79.1	79.6	80.7	80.0	78.6	78.2	0.7	1.9	1.1	0.7	1.1
	53.1	54.0	52.7	52.3	53.1	53.7	1.8	0.6	1.4	0.1	1.1
	44.4	44.9	46.0	43.7	43.9	43.4	1.0	3.5	1.5	1.2	2.2
	30.2	29.6	30.4	29.1	30.5	29.8	2.2	0.8	3.6	0.9	1.3
	21.0	20.6	20.6	20.1	20.8	21.5	1.9	1.8	4.1	1.0	2.5
	7.2	7.9	7.4	6.4	6.8	6.7	9.3	3.5	10.8	5.7	6.9

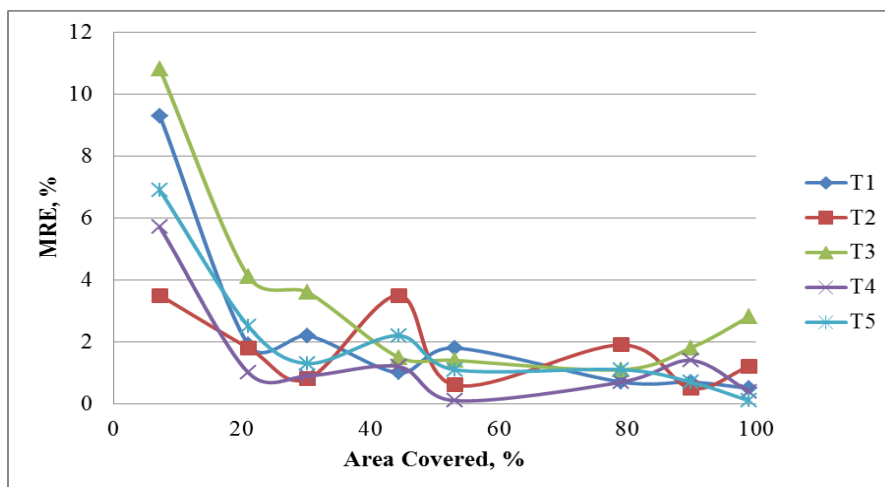


Figure 10. MRE after correction

Accuracy was increased dramatically across all algorithms after implementing the error correction formulas, where T4 exhibited the most accurate algorithm for dust detection. However, the error-correction formulas are only applicable to the specific solar panel model used in the test because other solar panel models will have different surface profiles.

4. Conclusion and future work

This paper demonstrates the practical application of different image processing techniques as an alternative, low cost, and non-invasive method of measuring dust and soiling along solar panel surfaces. The tests conducted on this study show that the proposed image processing algorithms can identify dust colour and texture with great reliability, consistency and accuracy far better than the human eye. Overall, the T4 (Image Matching) algorithm proved to be the most accurate on both controlled image and actual photograph tests.

Table 6. MRE before and after implementing error corrections on the actual image test

Image	Pixels changed (%)	MRE - Initial Results (%)					MRE - After Correction (%)				
		T1	T2	T3	T4	T5	T1	T2	T3	T4	T5
	98.9	0.7	0.4	0.7	1.0	1.0	0.5	1.2	2.8	0.4	0.1
	89.9	2.9	3.0	5.4	1.2	3.1	0.7	0.5	1.8	1.4	0.7
	79.1	4.5	5.8	5.5	3.4	6.4	0.7	1.9	1.1	0.7	1.1
	53.1	11.7	9.9	6.2	9.8	19.8	1.8	0.6	1.4	0.1	1.1
	44.4	14.5	16.0	7.8	12.0	24.1	1.0	3.5	1.5	1.2	2.2
	30.2	21.2	22.2	10.7	21.2	37.5	2.2	0.8	3.6	0.9	1.3
	21.0	30.8	30.1	16.1	29.0	50.2	1.9	1.8	4.1	1.0	2.5
	7.2	62.3	60.5	37.8	57.5	76.9	9.3	3.5	10.8	5.7	6.9

For future work, the Image Processing Toolbox will be streamlined to other solar panel types. Enhancements could be added on the Image Processing Toolbox to include features such as providing options for the user to select from a list of solar panel types and a gallery of dust types. The algorithms can then be fine-tuned by applying the appropriate error-correction formulas based on the user selection. The techniques could also be improved to include signal-based processing to detect other objects found on solar panel surfaces such as fauna droppings and small rocks. The techniques may possibly have other applications apart from dust detection and analysis and may be applicable on other systems in addition to solar panels.

The development of the Image Processing Toolbox provides a convenient tool in quickly acquiring dust and soiling measurements. Future applications of the software include integration of the algorithms into custom imaging devices designed to get real-time measurements and analysis. The algorithms can also be re-written for mobile devices such as smart phones and tablets to utilize the built-in cameras. Since most of the solar panel installations are mounted on rooftops, there is a possibility that solar panel analysis in the future can be performed by remotely controlled flying drones equipped with lightweight high definition cameras whose photographs can be processed directly by the Image Processing Toolbox programmed within the tiny onboard computer. This eliminates the exposure of technicians to certain hazards in accessing solar panels on rooftops. And with the imminent increase in uptake of PV systems in the Northern Territory, the Image Processing Toolbox will be a useful support tool for people working within the solar energy industry.



References

- Biryukov, S., Faiman, D., and Goldfeld, A., 1999. 'An optical system for the quantitative study of particulate contamination on solar collector surfaces.' *Solar Energy*, 66, p371–378.
- Blanchart, P., Ferecatu, M., Cui, S., and Datcu, M., 2014. 'Pattern retrieval in large image databases using multiscale coarse-to-fine cascaded active learning.' *IEEE Journal Of Selected Topics In Applied Earth Observations And Remote Sensing*, 7.
- Elbehiery, H., Hefnawy, A., and Elewa, M., 2007. 'Surface defects detection for ceramic tiles using image processing and morphological techniques.' *International Journal of Computer, Electrical, Automation, Control and Information Engineering*, 1, p1462-1466.
- Haralick, R., Shanmugam, K., and Dinstein, I. H., 1973. 'Textural features for image classification' *IEEE Transactions on Systems, Man and Cybernetics*, 3, p610-621.
- Kistner, M., Jemwa, G. T., and Aldrich, C., 2013. 'Monitoring of mineral processing systems by using textural image analysis.' *Minerals Engineering*, 52, p169-177.
- Lee, H. Y., 2014. 'Generation of photo-mosaic images through block matching and color adjustment.' *International Journal of Computer, Electrical, Automation, Control and Information Engineering*, 8, p440-443.
- Ndiaye, A., Kébé, C., Ndiaye, P., Charki, A. R., Kobi, A., and Sambou, V., 2013. 'Impact of dust on the photovoltaic (PV) modules characteristics after an exposition year in Sahelian environment: The case of Senegal.' *International Journal of Physical Sciences*, 8, p1166-1173.
- Parker, J. R. and Terzidis, K., 2011. 'Algorithms for image processing and computer vision.' Second Edition. Indianapolis. Wiley Publishing.
- Perez, P., Hue, C., Vermaak, J., and Gangnet, M., 2002. 'Color-based probabilistic tracking.' *7th European Conference on Computer Vision*, 2350, p661–675.
- Prakongkep, N., Suddhiprakarn, A., Kheoruenromne I., and Gilkes, R. J., 2010. 'SEM image analysis for characterization of sand grains in Thai paddy soils' *Geoderma*, 156, p20-31.
- Proietti, A., Leccese, F., Caciotta, M., Morresi, F., Santamaria, U., and Malomo, C., 2014. 'A new dusts sensor for cultural heritage applications based on image processing.' *Sensors*, 14, p9813-9832.
- Qasem, H., Betts, T. R., Müllejans, H., Albusairi, H., and Gottschalg, R., 2014. 'Dust-induced shading on photovoltaic modules.' *Progress in Photovoltaics: Research and Applications*, 22, p218-226.
- Sarver, T., Al-Qaraghuli, A., and Kazmerski, L. L., 2013. 'A comprehensive review of the impact of dust on the use of solar energy: History, investigations, results, literature, and mitigation approaches.' *Renewable and Sustainable Energy Reviews*, 22, p698-733.
- Singh, V., Singh, T. N., and Singh, V., 2010. 'Image processing applications for customized mining and ore classification.' *Arabian Journal of Geosciences*, 4, p1163-1171.
- Williams, A. T., Wiltshire, R. J., and Thomas, M. C., 1998. 'Sand grain analysis, image processing, textural algorithms and neural nets.' *Computers & Geosciences*, 24, p111-118.
- Yap, W. K., Baig, M., and Halawa, E., 2014. 'Performance monitoring and evaluation of a CIGS roof-integrated photovoltaic system under the unique tropical environment of Darwin, Northern Territory.' *2014 Asia-Pacific Solar Research Conference*, Sydney, Australia.
- Zhang, J. and Subasinghe, N., 2012. 'Extracting ore texture information using image analysis.' *Mineral Processing and Extractive Metallurgy*, 121, p123-130.